Journal of Scientific & Industrial Research
Vol. 85, June 2026, pp. 501-510
DOI: 10.56042/jsir.v85i6.31436

Enhanced Thermal Management of Lithium-Ion Batteries Using PCM and Nano-Enhanced PCM: A Comparative Study

P. S. N. Masthan Vali[1], Lakshmi Sirisha Maganti[1]*, Shital Y. Solanke[2], Govindarajan Murali[3], Rupendra Sharad Nehete[4] & Anant Sidhappa Kurhade[5,6]*

[1]Department of Mechanical Engineering, SRM University-AP, Amaravathi 522 240, Andhra Pradesh, India

[2]Department of Mathematics, School of Science and Humanities, Ramdeobaba University, RamdeobabaTekdi, Katol Road, Nagpur – 440 013, Maharashtra, India

[3]Department of Mechanical Engineering, Koneru Lakshmaiah Education Foundation, Vaddeswaram, Guntur, Andhra Pradesh 522 302, India

[4]Department of Mechanical Engineering, Indira College of Engineering and Management, Parandwadi, Pune, 410 506, Maharashtra, India

[5]Department of Mechanical Engineering, Dr. D. Y. Patil Institute of Technology, Sant Tukaram Nagar, Pimpri, Pune — 411 018, Maharashtra, India

[6]Dnyaan Prasad Global University (DPGU), School of Technology and Research — Dr. D. Y. Patil Unitech Society, Sant Tukaram Nagar, Pimpri, Pune, 411 018, Maharashtra, India

Received 12 May 2026; revised 14 August 2026; accepted 27 August 2026

Battery thermal management systems are essential to ensure the safety, capacity and lifespan of lithium-ion batteries for on-board use in electric vehicles. This study proposes a new 3D numerical model to investigate the thermal performance of a 24-cell battery pack consisting with various discharge power rates and 30°C ambient temperature. The numerical and experimental results showed good agreement, with percentage errors ranging from 0.32% to 7.55% across the nine cases. Without cooling, the maximum battery temperature reached 59.6°C at 3C, exceeding the recommended operating range. Phase Change Material (PCM) cooling reduced the peak temperature to 55.02°C, while Nano enhanced PCM further reduced it to 50.84°C. Nano enhanced PCM also improved temperature uniformity within the battery module by enhancing heat absorption and dissipation. The superior performance of Nano enhanced PCM is attributed to its enhanced effective thermal conductivity compared with conventional PCM. Overall, the results demonstrate that Nano enhanced PCM-based Battery Thermal Management System (BTMS) provides better thermal regulation than conventional PCM and offers a promising approach for safe and reliable Lithium-Ion Batteries (LIB) operation under high discharge conditions.

Keywords: Heat transfer, Nanofluid cooling, Natural convection, Thermal conductivity, Thermal management

Introduction

Due to its high energy density, long cycle life and excellent working ability, LIBs are widely used in portable electronics and electric vehicles. These benefits notwithstanding, an effective thermal control is still a critical challenge during high-power operation and under adverse surroundings. Overheating is detrimental to battery performance, boosts capacity decay rates; it also raises the risk of safety hazards (thermal runaway). It is hence considered a key thermal management solution, which led to the substantial interest in PCMs recently. By absorbing and releasing tempered latent heat during phase transitions, PCMs function to regulate battery temperature up to the desired operating range. This study explores the simulation-based optimization of PCM systems for enhancing the thermal performance of LIBs.

A PCM-based, cost-effective BTMS has also been pioneered to prevent the thermal runaway of the Electric Vehicle (EV) and Hybrid Electric Vehicle (HEV) battery packs when subjected to greater stress. The application of Newman Tiedemann Gu Kim (NTGK) electrochemical model in ANSYS shows the use of PCM significantly reduces cells highest temperature at larger rate and increase the uniformity on the battery thermal history. Results show that the PCM-based BTMS can control heat generation, thus alleviating the risk of thermal runaway. Internal heat generation caused by a variety of mechanisms such as electrochemical reaction kinetics, ohmic resistance, and entropic effects ultimately limits the operational

*Authors for Correspondence
E-mail: a.kurhade@gmail.com; lakshmisirisha.m@srmap.edu.in

performance of lithium-ion battery packs.[1,2] In addition to these major electrochemical contributors, internal mixing and phase transitions also generate residual heat that can be significant over time, so accurate characterization of their contributions is critical for determining individual cell temperature profiles to ultimately avoid thermal degradation.[3] Active air or liquid circulation tends to result in non-uniform temperature distribution with high discharge rates, which carries a risk of considerable energy loss and mechanical complexity.[4] Passive thermal management systems, in contrast to active ones, belong to a relatively stable and energy-efficient solutions using latent heat absorbance of phase change materials (PCMs) which are capable of controlling temperature.[5,6] Nevertheless, pristine organic phase change materials generally have a low thermal conductivity property that may lead to the creation of risk spots during high current discharges.[7] To overcome this limitation, abundant high-conductivity additives (e.g., graphene or alumina nanoparticles) have been utilized to improve the thermal transport regulation of the phase change medium, leading to a more even heat distribution throughout the pack.[8] The addition of nano-particles during the melting and crystallization processes creates an interface between the particles and matrix, which facilitates thermal energy transfer while improving thermal dissipation efficiency with enhanced effective thermal conductivity in composite, avoiding excessive heat generation by rapid charge-discharge transitions that can encounter the phenomenon of thermal runaway.[9,10] In addition, studies show that those phase change materials enhanced by the composite and nano-particles can limit cell temperature under 45°C in moderate to low discharge conditions with Deng gradients less than 5°C.[11] On the other hand, Nano-Enhanced Phase Change Material configurations provided increased thermal regulation capabilities at rate discharge cycles 3C (reduction of peak temperature increase by 21.3% with respect to bare cell architectures).[12] In addition to these performance improvements, the strategic integration of graphene-based enhancers has been shown to exhibit a synergistic interaction with latent heat storage capacity of the matrix material, dramatically mitigate transient temperature spikes during rapid 5C discharge events.[13] These improvements notwithstanding, while direct and indirect dispersions of these materials in paraffins appear promising, any practical approach will need to factor in their long-term chemical compatibility with the base paraffin; given that most solid lubricants become practically inactive due to sedimentation at extended duty cycles.[14] In addition, using metallic foams as the structural skeleton of the paraffin matrix or expanded graphite can effectively reduce sedimentation and significantly improve thermal conductivity, which helps to uniformly transfer heat to all parts within a module.[15,16] These advanced composites represent a breakthrough in heat dissipation rates (greater than 8 $W/m^2 \cdot K$) with over 90% of the base latent heat capacity preserved, thus improving the passive thermal buffering of the module.[17] Recent studies demonstrated that carbon-based fillers, such as Single-Walled Carbon Nanotubes (SWCNTs), could enhance the liquid fraction during phase change up to 66.5% and improve energy absorption subjected to transient thermal loads.[18] These improvements overcome the weakness of conventional PCMs on thermal conductivity and mechanical properties under high temperature conditions.[19,20] However, optimizing the nanofiller concentration is imperative to guarantee phase stability vs enhancing thermal conductivity while compromising latent heat capacity.[21,22] The experimental and numerical researches establish that the use of metallic structures or fins can improve their heat capacities in terms of slowing down the melting and lowering peak surface temperatures, within PCM composites.[23] Compared to conventional cylindrical cells and prismatic cells, they encourage more uniform heat transfer resulting in less local heating and aging in battery cells.[24,25] Thus, they not only assist to keep the battery module in a desired operating temperature; however, they prevent thermal runaway.[26,27] Pure paraffin has low thermal conduction at around 0.2 W/mK which can be enhanced through the inclusion of high-conductivity fillers (e.g., copper nanoparticles, metallic foams) reducing maximum cell temperature in high-rate charge–discharge cycles by more than 10% compared to pure paraffin.[28] These improvements in PCM design represent an important turning point towards developing passive systems that offer a combination of high latent heat storage and efficient thermal transport.[29,30] Nonetheless, integration of these advanced thermal management materials into battery architectures is key to enhance the overall cycle life and safety of battery cells for electric vehicles (EV).[31]

Future studies may focus on the long-term durability evaluations and scalable processes for manufacture of these composites which would be able to withstand practical vehicular operation without affecting the latent heat storage capacity.[32,33] In addition, upscaling from experimental prototypes to modular production-ready battery packs requires additional validation of how these nano-enhanced materials behave during the mechanical vibrations and thermal cycling associated with long-term operation in an electric vehicle.[34] Furthermore, tactile and digital twin technologies combined with these compositions is crucial to optimize thermal regulation mechanisms against particular battery pack geometry and operation profiles.[35] The work include the thermal insulation for battery thermal management[36], Phase Change Materials (PCM) based cooling methods[37], Artificial Intelligence (AI)-based thermal prediction and optimization methods, air cooling approaches and numerical assessment of battery pack cooling system.[38] The results of these studies show that thermal management can lower the temperature of batteries, hence improving the safety and performance of a battery pack in an EV.

During the last decade, BTMS utilizing PCM and Nano enhanced PCM have received attention, where higher latent heat and thermal conductivity tend to provide better performance. A numerical study is conducted to evaluate commercially available phase change materials (PCMs) having low melting points subjected to 1C, 2C and 3C discharge rates at an ambient temperature of 30°C in a comparison with air, PCM & Nano enhanced PCM cooling and therefore determine which PCM may be best suited for a particular condition.

This paper presents a comprehensive and validated comparison between conventional PCM and nano-enhanced PCM (Nano enhanced PCM) under the same operating conditions, which, to the best of the authors' knowledge, has not been reported in previous studies. In contrast to single-point or hybrid cooling studies, this analysis is performed with no cooling, PCM and Nano enhanced PCM in different discharge rates. This hybrid Nano enhanced PCM, which consists of the addition of graphene with Multi-Walled Carbon Nanotubes (MWCNTs) and graphite improves the thermal conductivity and stability. At 3C, the peak temperature was decreased from 55.02°C for PCM to 50.84°C with Nano enhanced PCM and also improved thermal uniformity and a good fit between numerical and experimental results were achieved. This integrated solution offers a comprehensive analysis of Nano enhanced PCM for battery thermal management.

Problem Description

This paper investigates the natural air cooling and passive PCM-based Battery Thermal Management System (BTMS) for 24 cylindrical ICR18650-26FM lithium-ion batteries. The height, diameter, and spacing of each cell are respectively 65 mm, 18 mm, and the distance between two adjacent cells is 3 mm in a pure nickel strip based (6S4P) packaging. The battery pack is simulated as depicted in Fig. 1. This study uses commercially available Paraffin Wax (PW) and nanoenhanced PCM as thermal management materials, with aluminium being used for the container material. The thermophysical properties of both the battery cells, PCM and aluminium are given in Table 1.

Graphene is a two-dimensional carbon-based material with excellent thermal conductivity and good mechanical strength, which can further enhance the thermal conductivity of Nano enhanced PCM and ensure efficient heat dissipation during battery operation. MWCNTs used specifically to provide stability and thermal scenario that further improve the mechanical and thermal conductivity thus providing strength and robustness in battery module. The introduction of graphite synthetic powder (GSP) imparts leak-proof properties and potential enhancement in the sensing metric and reversible capacity/cycling stability. GSP was therefore incorporated into the Nano enhanced PCM in this study. In conclusion, the synergistic effect of reducing thermal resistance through these materials improves convective and conductive heat transfer, as well as material stability

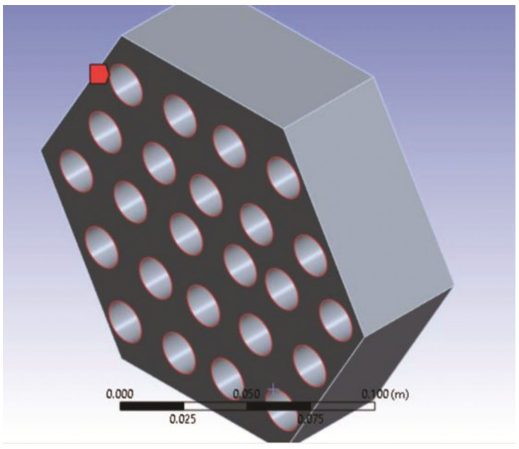


Fig. 1 — Three-dimensional model of the 24-cell lithium-ion battery pack (6S4P configuration)

Table 1 — Thermo physical properties of the materials used in the battery thermal management system

Parameter	Battery Cell	Aluminium	PCM (Paraffin Wax)	Nano enhanced PCM
Density (kg/m³)	2700	2710	820	910
Specific heat (J/kg·K)	900	897	2350	2180
Thermal conductivity (W/m·K)	3.8	237	0.32	18.5
Melting temperature (°C)	—	—	48–52	48–52
Dynamic viscosity (kg/m·s)	—	—	0.0048	0.0052
Thermal expansion coefficient (1/K)	—	—	0.00028	0.00022
Latent heat (kJ/kg)	—	—	178	165

to ensure good overall utilization of battery thermal characteristic.

Nano enhanced PCM was prepared from PW as base PCM and graphene, MWCNTs and GSP (synthetic graphite powder) as nano-additives. Nano-additive concentration was 1 wt.%, with 99 wt.% paraffin wax. The carbon-based fillers served to improve heat conduction, thermal stability, and strengthening properties but at the same time reduced leakage in phase change. As a result, the Nano enhanced PCM exhibited a thermal conductivity of 18.5 W/m·K, whereas pure paraffin presented only 0.32 W/m·K. The 1% loading was selected to improve thermal transport while preserving latent-heat storage capacity and avoiding excessive agglomeration or PCM reduction.

Numerical Modelling

Governing Equations

The transient thermal behaviour of the lithium-ion battery pack and PCM system is described using the conservation equations of mass, momentum, and energy. The following equations are used in the numerical model.

Continuity Equation

The continuity equation as explained in Eq. (1) in BTMS ensures the conservation of mass in the cooling fluid by balancing the rate of change of fluid density with the flow rate. It maintains system stability, preventing fluid buildup or depletion within the system. The momentum equations are explained in Eqs. (2)–(3). The energy equation, enthalpy formulation equation, sensible enthalpy are explained in in Eqs. (4)–(7).

$$\frac{\partial \rho}{\partial t} + \nabla.(\rho u) = 0 \quad \ldots (1)$$

where, ρ = density, u = velocity vector.

Momentum Equation

$$\frac{\partial(\rho u)}{\partial t} + \nabla.(\rho u u) = -\nabla p + \nabla.(\mu \nabla u) + \rho g + S_m \quad \ldots (2)$$

where, p = pressure, μ= dynamic viscosity, g = gravitational acceleration,S_m= momentum source term.

For natural convection, the buoyancy force can be expressed using the Boussinesq approximation

$$\rho g \approx \rho_0 g[1 - \beta(T - T_0)] \quad \ldots (3)$$

where, β = thermal expansion coefficient, T = is the local temperature,T_0= reference temperature.

Energy Equation

$$\frac{\partial(\rho h)}{\partial t} + \nabla.(\rho u h) = \nabla.(k \nabla T) + S_Q \quad \ldots (4)$$

where, h= total enthalpy, k = thermal conductivity, S_Q= volumetric heat-generation rate.

Enthalpy Formulation for PCM

The phase transition of paraffin PCM is modelled using the enthalpy method. The total enthalpy is calculated using Eq. (5),

$$h = h_s + \lambda L \quad \ldots (5)$$

where, h_s= sensible enthalpy, λ = liquid fraction, L = latent heat of fusion.

The sensible enthalpy,

$$h_s = h_{ref} + \int_{T_{ref}}^{T} C_p \, dT \quad \ldots (6)$$

For a PCM undergoing melting between the solidus and liquidus temperatures, the liquid fraction is expressed as,

$$\lambda = \begin{cases} 0 & T < T_s \\ \frac{T - T_s}{T_l - T_s}, & T_s \le T \le T_l \\ 1 & T > T_l \end{cases} \quad \ldots (7)$$

where, T_s = solidus temperatures,T_l = liquidus temperatures.

Battery Heat Generation

The heat generated inside each battery cell during discharge is introduced as a volumetric heat source and calculated using Eq. (8):

$$\dot{q}''' = \frac{\dot{Q}}{V_b} \quad \ldots (8)$$

where, $\dot{Q}$ = total heat generation rate, V_b = battery-cell volume.

For the present study, the volumetric heat-generation rates corresponding to 1C, 2C, and 3C discharge conditions are 10447, 41788.37, and 94023.84 W/m³, respectively, as specified in the manuscript.

The energy equation inside the battery is explained in Eq. (9),

$$\rho_b C_{p,b} \frac{\partial T_b}{\partial t} = \nabla.(k_b \nabla T_b) + \dot{q}''' \quad \ldots (9)$$

where, the subscript b denotes the battery.

Thermal Interface Conditions

At the battery–PCM interface, conservation of heat flux is shown in Eq. (10),

$$-k_b \frac{\partial T_b}{\partial n} = -k_{PCM} \frac{\partial T_{PCM}}{\partial n} \quad \ldots (10)$$

Similarly, at the PCM–aluminium container interface is shown in Eq. (11),

$$-k_{PCM} \frac{\partial T_{PCM}}{\partial n} = -k_{Al} \frac{\partial T_{Al}}{\partial n} \quad \ldots (11)$$

At the external surface of the aluminium container, natural convection is represented in is shown in Eq. (12),

$$-k_{Al} \frac{\partial_T}{\partial n} = h\,(T_s - T_\infty) \quad \ldots (12)$$

where, h = natural-convection heat-transfer coefficient, T_s = surface temperature, and T_∞= ambient temperature.

The manuscript specifies an ambient temperature of 30°C and a natural-convection coefficient of 5 W/m² K.

Initially, the complete battery module is assumed to be at the ambient temperature as explained in is shown in Eq. (13),

$$T\,(x, y, z, 0) = T_o \quad \ldots (13)$$

where, $T_o = 30°C$

ANSYS 2024 R1 was used for the numerical analysis of thermal behaviour of battery module. A 3D computer-aided battery simulator created in Design Modeler, using tetrahedral meshed with 89795 elements. The continuity, momentum and energy equations were solved using the finite volume method considering the phase-change behaviour of PCM and Nano enhanced PCM. The ambient temperature is 30°C with natural convection and transient simulations were performed at 1C, 2C and 3C discharge rates.

Grid size of 89795 elements and a 1 s time step produced accurate temperature predictions with acceptable computational cost and were therefore selected for additional simulations. The experimental results were in good accordance with the numerical model.[35] The higher the discharge rate, the higher the battery temperature, but Nano enhanced PCM successfully kept the battery temperature below 50°C. Compared with conventional PCM, Nano enhanced PCM achieved a peak temperature reduction of up to 8.81% and an inter-module temperature difference reduction of up to 91.48%, showing more efficient and uniform thermal management.

The discharge time of the battery pack was defined in accordance with the specified discharge condition and thermal safety limits associated with the battery cells. All the experiments were performed using the temperature measurement system to continuously monitor the cell temperature. The battery was found to be a safer rechargeable one which would stop discharging once it reaches the safety point or suffer thermal run away. The 2C discharge test was intentionally stopped at about 1800 s to avoid overheating (though the measured discharge time under this experimental condition was 1142.56 s) so that the discharged time indicatively stated here represents the actual duration in which the appropriate discharge conditions sustained, whereas 1800 s value is a safety limit on maximum allowable test duration

Hence, the discharge termination criterion in this research was predominantly on a temperature basis as opposed to voltage or state of charge. This same consideration was taken during the experimental measurements, by avoiding exposing cells to temperatures that would restrict safety and performance.

Results and Discussion

Three LIB module thermal management conditions were simulated in the second ANSYS analysis. The first case is without cooling mode use at ambient temperature of 30°C, the heat dissipation character of the 18650 cylindrical cells is limited in local area leading to non-uniform temperature distributions create high temperatures at centre of battery pack than outside cells. In the second instance, passive cooling medium was placed as a PCM to absorb heat generated by battery operation that resulted in uniform temperature and lower thermal gradients. For the third case, PCM was enhanced with metals on a nano-range to increase heat absorption and loss.

Discharge Rate Effects on the LIB Pack without Cooling

At a 1C discharge rate, Fig. 2 shows that the simulated peak temperature of the LIB module reached 54.27°C, compared with 52.55°C experimentally. As shown in Fig. 3a, the middle region heated faster than the corners, resulting in a non-uniform temperature distribution and exceeding the recommended 50°C limit. The discharge time was 3433.47 s. At 2C, the simulated and experimental peak temperatures were 59.30°C and 55.90°C, respectively. The battery temperature approached 60°C at 1140 s, and the discharge was stopped at 1800 s to prevent overheating as shown in Fig. 3b. The actual discharge time was 1142.56 s. At 3C, the simulated peak temperature was 59.60°C, while the experimental value was 55.10°C. The battery reached nearly 60°C within 540 s, with a discharge duration of 539.82 s as shown in Fig. 3c. These results demonstrate that higher discharge rates cause faster temperature rise, highlighting the need for effective thermal management.

Discharge Rate Effects on the LIB Pack with PCM Cooling

With PCM cooling, Fig. 4 shows that at a 1C discharge rate, the simulated and experimental peak temperatures were 50.8°C and 49.18°C, respectively. As shown in Fig. 5a, PCM cooling reduced the temperature rise and maintained the battery near the safe operating range. The corresponding discharge time was 3519.84 s. At 2C, the simulated peak temperature was 49.6°C, while the experimental value was 52.12°C. PCM cooling effectively restricted the temperature rise despite the higher discharge rate, with a discharge time of 1765.07 s as shown in Fig. 5b. At 3C, the simulated and experimental peak temperatures were 55.02°C and 54.38°C, respectively. As shown in Fig. 5c, PCM cooling controlled the temperature increase, with a discharge time of 904.86 s. The close agreement between numerical and experimental results confirms the effectiveness of PCM cooling for controlling battery temperature under different discharge conditions.

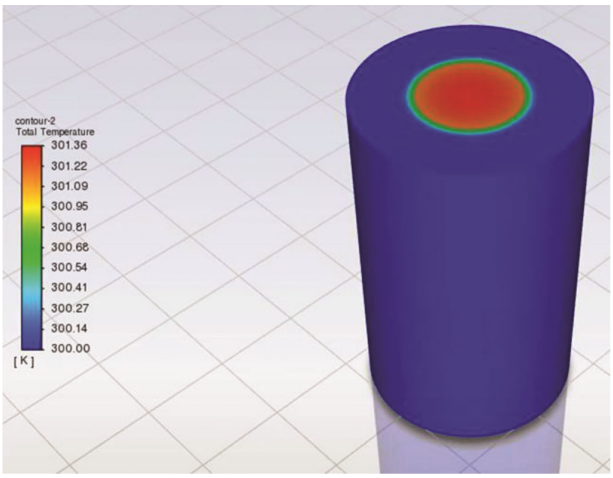


Fig. 2 — Temperature contour of a single cell without cooling

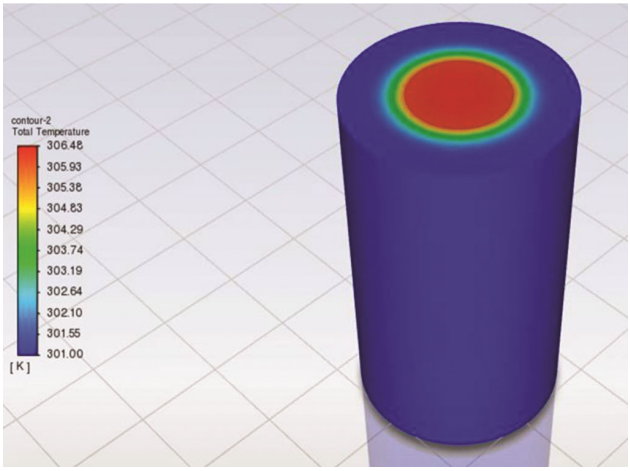


Fig. 4 — Temperature contour of a single cell with PCM cooling

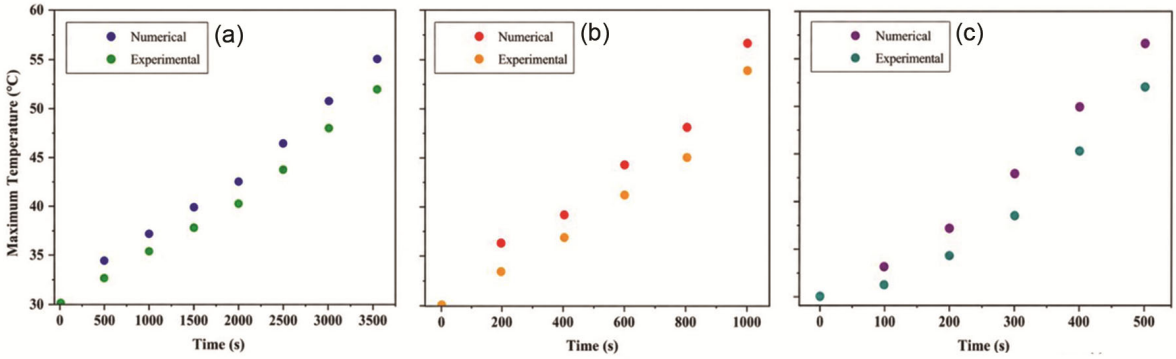


Fig. 3 — Comparison of numerical and experimental maximum temperature profiles at (a) 1C, (b) 2C and (c) 3C discharge rate without cooling

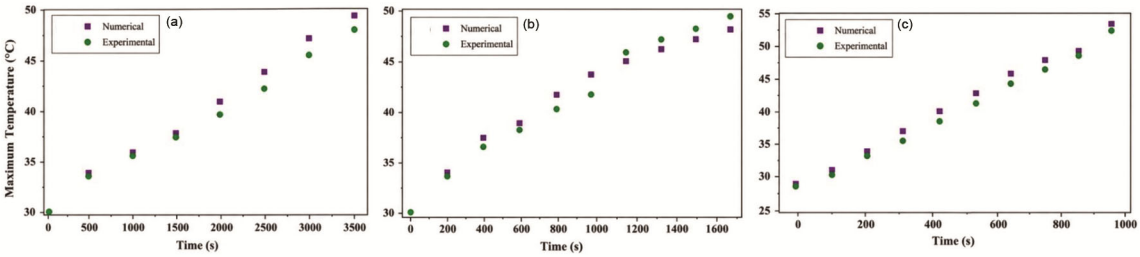


Fig. 5 — Comparison of numerical and experimental maximum temperature profiles at (a) 1C, (b) 2C and (c) 3C discharge rate with PCM cooling

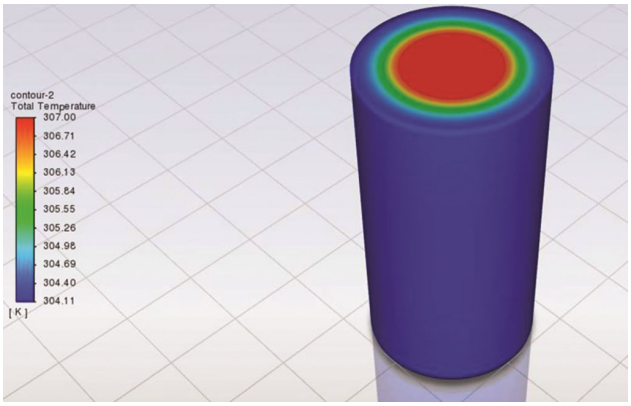


Fig. 6 — Temperature contour of a single cell with Nano enhanced PCM cooling

Discharge Rate Effects on the LIB Pack with Nano Enhanced PCMCooling

With Nano enhanced PCM cooling, Fig. 6 shows the overall thermal performance, while Figs. 7 (a–c) presents the corresponding temperature profiles at 1C, 2C, and 3C discharge rates. At 1C, the simulated and experimental peak temperatures were 47.28°C and 45.89°C, respectively, with a discharge time of 3436.73 s. At 2C, the corresponding temperatures were 47.89°C and 47.74°C, with a discharge time of 1739.51 s. At 3C, the simulated and experimental peak temperatures reached 50.84°C and 49.53°C, respectively, with a discharge time of 902.077 s. The close agreement between numerical and experimental results confirms the reliability of the Nano enhanced PCM model. Overall, Nano enhanced PCM effectively controlled the temperature rise at higher discharge rates and maintained the battery within a relatively safe thermal range.

Experimental Uncertainty and Statistical Error Analysis

The fitness between the numerical and experimental results was quantitatively assessed by examining the maximum temperatures acquired under different discharge rates of 1C, 2C, and 3C for uncooled, PCM, and Nano enhanced PCM. Percentage error was computed using the following Eq. (14),

$$\text{Percentage Error (\%)} = \left|\frac{T_{num}-T_{exp}}{T_{num}}\right| \times 100 \quad \ldots (14)$$

where, T_{num} = maximum temperature predicted by the numerical model, T_{exp} = corresponding experimentally measured maximum temperature.

The absolute temperature difference was calculated using Eq. (15),

$$\Delta T = \left|T_{num} - T_{exp}\right| \quad \ldots (15)$$

where, T_{num}= maximum temperature predicted by the numerical model, T_{exp} = corresponding experimentally measured maximum temperature.

The comparison of the numerical and experimental maximum temperatures is presented in Table 2.

The percentage error of these calculations ranged from 0.31% to 8.17%, indicating good agreement between the numerical and experimental results. The minimum deviation of 0.31% was observed for the Nano-enhanced PCM condition at 2C, while the maximum deviation of 8.17% occurred under the uncooled condition at 3C. For the Nano-enhanced PCM cases, the errors were 3.03%, 0.31%, and 2.64% at 1C, 2C, and 3C, respectively. The global Mean Absolute Percentage Error (MAPE) across the nine cases was approximately 3.65%. These results demonstrate that the numerical model provides a reliable prediction of the thermal behaviour of the battery pack under the investigated discharge and cooling conditions.

Maximum Temperature Difference of the Lithium-Ion Battery Pack at Three Different Discharge Rates

The bar graph in Fig. 8 compares the numerical–experimental temperature deviation for the different cooling configurations at 1C, 2C, and 3C discharge rates. The percentage deviation was calculated using the experimental temperature as the reference value. Without cooling, the deviation increased from 3.27% at 1C to 6.08% at 2C and 8.17% at 3C. With PCM cooling, the corresponding deviations were 3.29%,

Table 2 — Comparison of numerical and experimental maximum temperatures

Cooling condition	Discharge rate	Numerical T_{num} (°C)	Experimental T_{exp} (°C)	ΔT (°C)	Error (%)
Without cooling	1C	54.27	52.55	2.17	3.27
Without cooling	2C	59.30	55.90	3.40	6.08
Without cooling	3C	59.60	55.10	4.50	8.17
PCM	1C	50.80	49.18	1.62	3.29
PCM	2C	49.60	52.12	2.52	4.83
PCM	3C	55.02	54.38	0.64	1.18
Nano enhanced PCM	1C	47.28	45.89	1.39	3.03
Nano enhanced PCM	2C	47.89	47.74	0.15	0.31
Nano enhanced PCM	3C	50.84	49.53	1.31	2.64

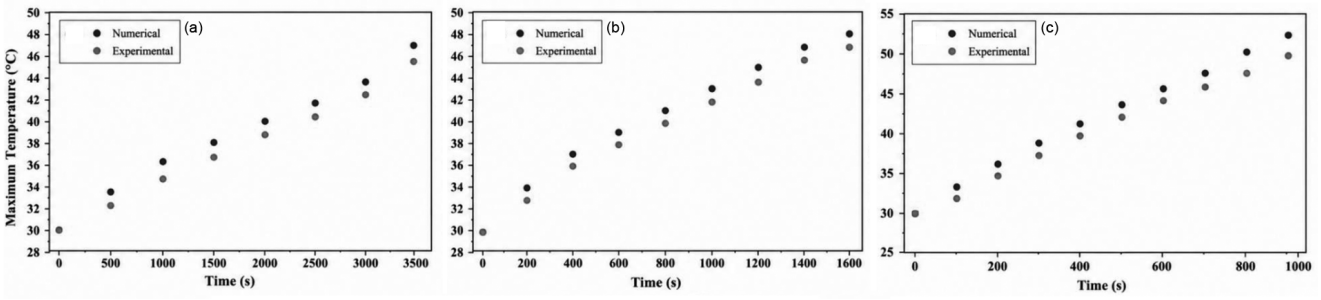


Fig. 7 — Comparison of numerical and experimental maximum temperature profiles at (a) 1C, (b) 2C and (c) 3C discharge rate with Nano enhanced PCM cooling

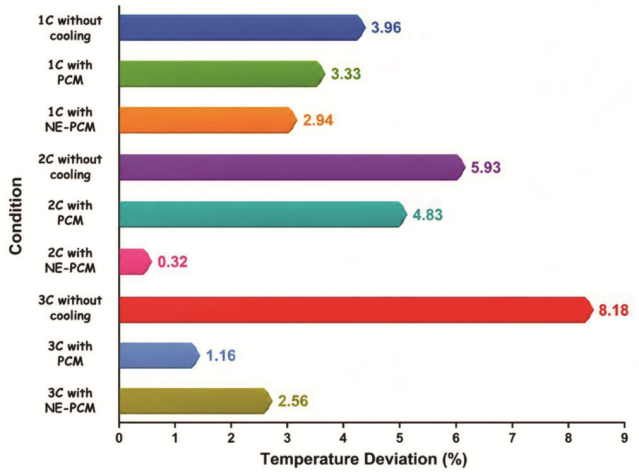


Fig. 8 — Maximum temperature deviation under different cooling conditions

4.83%, and 1.18%, respectively. Nano-enhanced PCM produced deviations of 3.03%, 0.31%, and 2.64% at 1C, 2C, and 3C, respectively. The results indicate good agreement between the numerical and experimental temperatures, with the lowest deviation observed for Nano-enhanced PCM at 2C.

Conclusions

This study investigated the thermal performance of a 24-cell 18650 lithium-ion battery pack cooled using PCM and nanoenhanced PCM under 1C, 2C, and 3C discharge rates. Without cooling, peak temperatures reached 54.27°C, 59.30°C, and 59.60°C, respectively. Extended PCM reduced these temperatures to 50.8°C, 49.6°C, and 55.02°C, while nanoenhanced PCM achieved the lowest values of 47.28°C, 47.89°C, and 50.84°C. The nanoenhanced PCM reduced peak temperature by approximately 7–9°C compared with the uncooled condition, particularly at higher discharge rates, demonstrating improved heat absorption and temperature regulation. The numerical results showed good agreement with experimental measurements, with percentage errors ranging from 0.31% to 8.17% across the nine tested cases. Overall, nanoenhanced PCM provided superior thermal performance compared with conventional PCM and represents a promising cooling approach for maintaining safer operating temperatures in lithium-ion battery packs under high discharge conditions.

Conflicts of Interest

The authors declare that they haveno conflict of interest.

Acknowledgement

The authors greatly acknowledge SRM University for providing the infrastructure facilities to perform the experiments and for support in analysis part.

Reference

1 Mahmud M, Rahman K S, Rokonuzzaman Md, Habib A K M A, Islam Md R, Motakabber S M A, Channumsin S & Chowdhury S, Lithium—ion battery thermal management for electric vehicles using phase change material: A review, *Results Eng*, **20** (2023) 101424, doi:10.1016/j.rineng. 2023.101424.

2 Togun H, Basem A, Jweeg M J, Anqi A E, Alshamkhani M T, Chattopadhyay A K, Sharma B K, Niyas H, Biswas N, Sadeq A M & Alhassan MS , Revolutionizing battery thermal management: Hybrid nanofluids and PCM in cylindrical pack cooling, *Mater Renew Sustain Energy*, **14(2)** (2025), doi:10.1007/s40243-025-00313-x.

3 Ramprabu J, Kandasamy V & Vairavel M, Optimizing lithium—ion battery thermal management using CFD and nano–cooling, *TEH VJESN*, **32(3)** (2025), doi:10.17559/tv-20240522001645.

4 Rashid F L, Al Obaidi M A, Maimuri N M L A, Ashour A M, Ahmad S, Ameen A, Kadhim S A, Hammoodi K A, Khudhayer W J & Altaee A, Advancements in thermal management of lithium-ion batteries: the role of nanofluids and phase change materials, *Environ Technol Rev*, **15(1)** (2026) 40–75, doi:10.1080/21622515.2025.2609810.

5 Rasool G, Wang X, Sun T, Hayat T, Sheremet M A, Uddin A, Shahzad H, Abbas K, Razzaq I & Yuexin W, Recent advancements in battery thermal management system (BTMS): a review of performance enhancement techniques with an emphasis on nano-enhanced phase change materials, *Heliyon*, **10(17)** (2024), doi:10.1016/j.heliyon.2024.e36950.

6 Bandela R & Shaik F, Numerical investigation of passive thermal management of batteries in electric vehicle using nano enhanced phase change materials, *Heat Transf*, **55(3)** (2026), doi:10.1002/htj.70166.

7 Kurhade A S, Siraskar G D, Dalvi S A, Kharat P V, Jadhav N A, Shelkande V D, Murali G, Waware S Y & Yadav R S, Passive cooling of EV batteries using phase change material: A simulation study, *J Mines Met Fuels*, **73(2)** (2025) 447–454, doi:10.18311/jmmf/2025/47368.

8 Pranto M M H, Adit Md A & Bari Y A, Thermal management of lithium-ion batteries using fin–integrated nano-enhanced PCM under forced air convection: A CFD study, *Next Energy*, **11** (2026) 100561, doi:10.1016/j.nxener. 2026.100561.

9 Dilbaz F, Selımefendıgıl F & Öztop H F, Comparisons of different cooling systems for thermal management of lithium-ion battery packs: phase change material, nano–enhanced channel cooling and hybrid method, *J Energy Storage*, **90** (2024) 111865, doi:10.1016/j.est.2024.111865.

10 Yaw C T, Rajamony R K, Bhutto Y A, Bakthavatchalam B, Kottala R K, Chopra K, Paw J K S, Doroody C, Allasi H L & Soudagar M E M, Two phase heat transfer approaches for battery thermal management: current status, challenges and future outlook, *Res Eng*, **27** (2025) 105749, doi:10.1016/j.rineng.2025.105749

11 Shruti G, Salunkhe P B & Shenoy B S, Recent progress on passive cooling strategies for li-ion battery of electric vehicles, *J Energy Storage*, **156** (2026) 121550, doi:10.1016/ j.est.2026.121550.

12 Hadawale P R & Sathe A, Passive battery thermal management of lithium-ion battery using nano-enhanced phase change material: an experimental study, *Eng Res Express*, **7(2)** (2025) 25510, doi:10.1088/2631-8695/adc4c0.

13 Rahmanian S, Rahmanian K H & Hosseinzadeh K H, Thermal management in high-power lithium-ion batteries: synergistic effects of phase change material thickness, graphene enhancers, and active cooling systems, *Case Stud Therm Eng*, **74** (2025) 106771, doi:10.1016/j.csite.2025. 106771.

14 Mallimoggala S, Advanced thermal management in aircraft lithium-ion battery packs: optimization of heat dissipation using heat spreaders and phase change materials, *J Therm Eng*, **11(5)** (2025) 1420–1438, doi:10.14744/thermal. 0000984.

15 Murali G, P S N Masthan V, Adduri S S M Sitaramamurty, Kurhade A S, Mohammed Al A, Ali K, Faris S B & Afzal A, Solid-state electrolytes for advanced solid-state batteries: a comprehensive review of materials, ionic conductivity, and interface engineering, *J Energy Storage*, (**180)** (2026) 124038, doi:10.1016/j.est.2026.124038.

16 Masthan V P S, Murali G & Kurhade A S, Simulation-based evaluation of battery thermal management systems for cylindrical li-Ion batteries in electric vehicles, *J Mines Met Fuels*, **73(3)** (2025) 555–570, doi:10.18311/jmmf/2025/ 48185.

17 Shivram S & Harish R, Impact of dual nano-enhanced phase change materials on mitigating thermal runaway in lithium-ion battery cell,*Case Stud Therm Eng*, **60**(2024) 104667, doi:10.1016/j.csite.2024.104667.

18 Vali P S N M & Murali G, Experimental study on thermal management of nano-enhanced phase change material integrated battery pack, *Heat Mass Transf*, **146(3)** 2023, doi:10.1115/1.4064155.

19 Wang J, Mao Y & Miljkovic N, Nano-enhanced graphite/phase change material/graphene composite for sustainable and efficient passive thermal management, *Adv Sci*, **11(38) (**2024) 2402190, https://www.ncbi.nlm.nih.gov/ pmc/articles/11481206.

20 Shamnaz M, Bal D K & Sahoo B B, Numerical simulation-guided assessment of modern composite phase-change materials for thermal regulation of 21700 lithium-ion battery modules under high-rate operation, *Res Eng*, **29 (**2026) 109756, doi:10.1016/j.rineng.2026.109756.

21 Luo J, Xia W, Wang S, Li D & Kang X, Comprehensive application of phase change materials in lithium-ion battery thermal management: from single cooling to coupled systems, *Energy Technol*, **13(8)** (2025) 2401930, doi:10.1002/ente.202401930.

22 Islam A, Pandey A K, Saidur R, Aljafari B & Tyagi V V, Advancements in foam-based phase change materials: unveiling leakage control, enhanced thermal conductivity, and promising applications, *J Energy Storage*, **74** (2023) 109380, doi:10.1016/j.est.2023.109380.

23 Prem K S, Krishnappa G B & Devegowda M, A comprehensive review on air-cooled battery thermal management system of electric vehicles, *J Therm Eng*, **12(2) (**2026) 830–841, doi:10.14744/thermal.0001116.

24 Zare P, Perera N, Lahr J & Hasan R, Solid-liquid phase change materials for the battery thermal management systems in electric vehicles and hybrid electric vehicles – A systematic review, *J Energy Storage*, **52** (2022) 105026, doi:10.1016/j.est.2022.105026.

25 Rao G A P & Kumar S S, A review of integrated battery thermal management systems for lithium-ion batteries of electric vehicles, e-*Prime Adv Electr Eng Electron Energy*, **8** (2024) 100526, doi:10.1016/j.prime.2024.100526.

26 Dolla D A & Fetene M G, Investigations of phase change materials in battery thermal management systems for electric vehicles: A review, *Mater Res Express*, **11(1)** (2023) 12002, doi:10.1088/2053–1591/ad1949.

27 Kang C, Yang J, Yuan X, Qiu C & Cai Y, A novel multilayer composite structure-based battery thermal management system, *Front Energy Res*, **11 (**2023) 1187904, doi:10.3389/fenrg.2023.1187904.

28 Calboréan A, Máthé L & Bruj O, Phase change materials for thermal management in lithium-ion battery packs: A review, *Batteries*, **11(12)** (2025) 432, doi:10.3390/batteries11120432.

29 Kibria Md G, Mohtasim Md S, Paul U K, Fahim I A, Nafi, Das B K & Mohammed H A, A Review on composite phase change materials and fins-based li-ion battery thermal management systems with design perspectives and future outlooks, *Energy Fuels*, **38(15)** (2024) 13637–13660, doi:10.1021/acs.energyfuels.4c02062.

30 Talebizadehsardari P, Hosseinzadeh K, Mohammed H I, Maarof H A, Rashid F L, Togun H, Biswas N, Miaari A A, Ali H M, Rocca A L, Sen S & Cairns A, Phase change materials in thermal management of li-ion batteries: A state-of-the-art review, *J Energy Storage*, **145 (**2025) 119782, doi:10.1016/j.est.2025.119782.

31 Vali M P, Govindarajan M & Chinnasamy S, Comparison study on cooling management of composite phase change material battery pack: Two different cases, *Therm Sci*, **27(6)** (2023) 4757–4765, doi:10.2298/TSCI220816218V.

32 Dandotiya D, Joshi A K, Kakati P & Sudharshan J, Incorporating copper and carbon nanotube nanoparticles into phase change materials for enhanced thermal management in Batteries, *J Mines Met Fuels*, **71(10) (**2023) 1799–1808, doi:10.18311/jmmf/2023/35045.

33 Masthan V PSN & Murali G, Battery thermal management system on trapezoidal battery pack withliquid cooling system utilizing phase change material, *J Heat Mass Transf*, **146(1)** (2024) 011003, doi:10.1115/1.4063355.

34 Suryavanshi S S, Ghanegaonkar P M, Wankhede S R & Kawade R K, An experimental study on the influence of environmental conditions on the temperature of the battery pack during discharge in an electric vehicle, utilising thermal insulating material, *Int J Ambient Energy*, **46(1)** (2025) 2503329, doi:10.1080/01430750.2025.2503329.

35 Patıl R & Desai A, Performance of phase changing material in an artificially created cold region to promote latent heat thermal energy storage, *J Therm Eng*, **7(7)** (2021) 1694–1703, doi:10.18186/thermal.1025935.

36 Barewar S D, Kalos P S, Bakthavatchalam B, Joshi M, Patil S & Sonekar M, Analysis and prediction of thermo-physical properties in water-based MWCNT-ZnO hybrid nanofluids using ANN and ANFIS models, *Int J Thermofluids*, **27** (2025) 101159, doi:10.1016/j.ijft.2025.101159.

37 Thombare S, Dhande H & Khedekar S, Hybrid electric vehicle thermal optimization using artificial intelligence based controller with super capacitor battery technology, *AIP Conf Proc*, **2842(1)** (2023) 020009, doi:10.1063/5.0175688.

38 Suryavanshi S, Ghanegaonkar P M & Wankhede S, An air-cooled cylindrical Li-ion 5×5 battery module with a novel flow-diverting arrangement and variable vent positions for electric vehicles: A numerical thermal analysis, *Heat Transf*, **54(1)** (2025) 203–222, doi:10.1002/htj.23172.